

# Simultaneous impacts of nuclear shell structure and collectivity on $\beta$ -decay: evidence from $^{80}\text{Ga}_{49}$

R. Li,<sup>1,2,\*</sup> D. Verney,<sup>1</sup> G. De Gregorio,<sup>3,4</sup> R. Mancino,<sup>5,6</sup> I. Matea,<sup>1</sup> L. Coraggio,<sup>3,4</sup> N. Itaco,<sup>3,4</sup> M. N. Harakeh,<sup>7</sup> C. Delafosse,<sup>1,8</sup> F. Didierjean,<sup>9</sup> L. A. Ayoubi,<sup>1,8</sup> H. Al Falou,<sup>10</sup> G. Benzoni,<sup>11</sup> F. Le Blanc,<sup>1</sup> V. Bozkurt,<sup>12</sup> M. Ciemala,<sup>13</sup> I. Deloncle,<sup>1</sup> M. Fallot,<sup>14</sup> C. Gaulard,<sup>1</sup> A. Gottardo,<sup>15</sup> V. Guadilla,<sup>14</sup> J. Guillot,<sup>1</sup> K. Hadyńska-Klęk,<sup>16</sup> F. Ibrahim,<sup>1</sup> N. Jovancevic,<sup>1,†</sup> A. Kankainen,<sup>8</sup> M. Lebois,<sup>1</sup> T. Martínez,<sup>17</sup> P. Napiorkowski,<sup>18</sup> B. Roussiere,<sup>1</sup> Yu. G. Sobolev,<sup>19</sup> I. Stefan,<sup>1</sup> S. Stukalov,<sup>19</sup> D. Thisse,<sup>1</sup> and G. Tocabens<sup>1</sup>

<sup>1</sup>Université Paris-Saclay, CNRS/IN2P3, IJCLab, 91405 Orsay, France

<sup>2</sup>KU Leuven, Instituut voor Kern- en Stralingsfysica, Celestijnenlaan 200D, B-3001 Leuven, Belgium

<sup>3</sup>Dipartimento di Matematica e Fisica, Università degli Studi della Campania "Luigi Vanvitelli", Viale Abramo Lincoln 5, I-81100 Caserta, Italy

<sup>4</sup>Istituto Nazionale di Fisica Nucleare, Complesso Universitario di Monte S. Angelo, Via Cintia, I-80126 Napoli, Italy

<sup>5</sup>Institut für Kernphysik (Theoriezentrum), Fachbereich Physik, Technische Universität Darmstadt, Schlossgartenstrasse 2, 64298 Darmstadt, Germany

<sup>6</sup>GSI Helmholtzzentrum für Schwerionenforschung, Planckstrasse 1, 64291 Darmstadt, Germany

<sup>7</sup>ESRIG, University of Groningen, Zernikelaan 25, 9747 AA Groningen, The Netherlands

<sup>8</sup>University of Jyväskylä, Department of Physics, Accelerator Laboratory, P.O. Box 35, FI-40014 University of Jyväskylä, Finland

<sup>9</sup>Institut Pluridisciplinaire Hubert Curien, CNRS/IN2P3 and Université de Strasbourg, Strasbourg, France

<sup>10</sup>Faculty of Sciences 3, Lebanese University, Michel Slayman Tripoli Campus, Ras Maska 1352, Lebanon

<sup>11</sup>INFN, sezione di Milano, Dipartimento di Fisica, Milano, Italy

<sup>12</sup>Nigde University, Science Faculty, Department of Physics, Nigde, Turkey

<sup>13</sup>Institute of Nuclear Physics, Polish Academy of Sciences, Krakow, Poland

<sup>14</sup>Subatech, CNRS/IN2P3, Nantes, EMN, F-44307, Nantes, France

<sup>15</sup>Laboratori Nazionali di Legnaro, I-35020 Legnaro, Italy

<sup>16</sup>Department of Physics, University of Oslo, Oslo, Norway

<sup>17</sup>Centro de Investigaciones Energéticas Medioambientales y Tecnológicas (CIEMAT), Madrid, Spain

<sup>18</sup>Heavy Ion Laboratory, University of Warsaw, 02-093 Warsaw, Poland

<sup>19</sup>Joint Institute for Nuclear Research, Dubna, Russia

(Dated: June 3, 2024)

The Gamow-Teller strength distribution covering the entire  $\beta$ -decay window, up to 10.312(4) MeV, of  $^{80g+m}\text{Ga}$  was measured for the first time in photo-fission of  $\text{UC}_x$  induced by 50 MeV electron beam. The new data show significant enhancement in the high-energy region with a jump-structure. Simultaneously, the  $\gamma$  de-exciting behavior of  $\beta$ -populated states presents a competition between de-excitation to  $2_1^+$  [ $\beta_2 = 0.155(9)$ ] and to  $2_2^+$  [ $\beta_2 = 0.053_{0.009}^{0.008}$ ] in  $^{80}\text{Ge}$ . Based on these facts and combined with a realistic shell model calculation and systematic analysis of logft ratio between precursor  $\beta$ -decay to  $2_2^+$  and to  $2_1^+$  of Ga isotopes, we conclude that these phenomena evidence simultaneous impacts of nuclear shell structure and collectivity on B(GT) and its distribution and, therefore, the half-life of the precursor. These data prove that the nucleus as a multi-nucleon correlated quantum system reacts as a whole when  $\beta$ -decay occurs in contrast to simple single-particle excitation. Additionally, the comparison with the theoretical results demonstrate how challenging is the description of the experimental data obtained, and render this experimental outcome a sound test for the theoretical models.

PACS numbers:

**Introduction.**  $\beta$ -decay keeps its mystery to some extent nowadays, more than one hundred and twenty years since its discovery in the nuclear medium, which is a self-organized many-body quantum system dominated by the strong interaction. This arises from complexity of the weak-interaction process in nuclei and the response of the nuclei following  $\beta$ -

transition. From classical Fermi current-current interaction theory, phenomenal effective field theory based on point-like interaction hypothesis, nuclear  $\beta$ -decay is a process of conversion of a neutron to a proton or vice versa. Consequently, it generates a one-particle one-hole (1p1h) excitation in daughter nuclei. Based on this theory, observables in nuclear  $\beta$ -

decay, mainly half-lives, can be reproduced approximately.

However, recent studies further reveal that the  $\beta$ -decay of atomic nuclei is not as simple as introduced above. This discovery was triggered, from the theoretical side, by precisely reproducing the B(GT) without using a phenomenological quenching factor [1–5] either through adding 2p2h correlations in the final-state wave function [6], or adding nuclear collective vibration in the final-state wave function [7], or including the two-body current contributions of the axial current in the  $\beta$ -decay operator [8, 9]. In all cases, multi-correlated excitation states must be populated instead of single-particle states. From the experimental side, the recent observation of  $\beta$ -populated Pygmy Dipole Resonance (PDR) components in  $^{80}\text{Ge}$  [10] supports this conclusion, which directly proved the existence of collective excitations in nuclear  $\beta$ -decay. Additionally, studies of B(GT) distributions using the total absorption gamma spectroscopy (TAS) technique [11–13] also indicate the influence of nuclear deformation in  $\beta$ -decay.

In this article, we report on the evidence of simultaneous impacts of nuclear shell structure and collectivity on  $\beta$ -decay properties via: 1) investigating the evolution of the cumulated B(GT) jump-structure with the excitation energy from both ground and isomeric state of  $^{80}\text{Ga}$ ; 2) comparison with theoretical results obtained within the framework of realistic nuclear shell model without using a phenomenological quenching factor of the axial coupling constant; 3) analyzing the decay patterns of excited states in the daughter nucleus; 4) trying to search for correlations between quadrupole deformation of the precursors and selectivity of  $\beta$ -population. In fact, one expects that, if a given precursor has a large quadrupole deformation, like  $^{80m}\text{Ga}$  with spin-parity  $3^-$ , it has a higher probability to decay to a collective state with higher deformation like  $2_1^+$  in  $^{80}\text{Ge}$  than to a state with almost spherical shape like  $2_2^+$  due to a larger overlap of their wave functions. Consequently, there is a lower logft value for decay to  $2_1^+$ .

$^{80}\text{Ga}$  decays to  $^{80}\text{Ge}$ , a nucleus that has  $Z=32$  protons and two neutron holes in the closed shell  $N=50$ . This decay has several unique characters that allow to investigate their impacts. Firstly, the neutron-rich nucleus  $^{80}\text{Ga}$  has a large  $Q_\beta$  value with 10.312(4) MeV [14] so that it offers a wide energy window to observe the excitation spectrum of  $^{80}\text{Ge}$ . Secondly, the structure of  $^{80}\text{Ge}$  is considered to be dominated by strong shell effects [15]. However, quadrupole and octupole deformations have also been observed [16]. Therefore, it is a good case to investigate the role of nuclear collectivity in  $\beta$ -decay particularly in the closed-shell region. In addition,  $^{80}\text{Ga}$  is known to have two  $\beta$ -decaying states [17]: the  $6^-$  ground state with a longer half-life of 1.91(3) s and the  $3^-$  isomeric state with a half-life of 1.57(1) s [10], at 22.4 keV excitation energy [18]. This makes that two precursors are  $\beta$ -feeding  $^{80}\text{Ge}$  simultaneously and producing more abundant spin states, given allowed and first-forbidden transitions, from 0 to 8 and, therefore, resulting in a rich observed structure.

*Experiment.* The experiment was performed at the Accelerator

Linear and Tandem at Orsay (ALTO) [19]. A radioactive  $^{80g+m}\text{Ga}$  ion beam was produced at the ALTO-ISOL facility using photo-fission of  $\text{UC}_x$  induced by a 50 MeV electron beam with an intensity of  $\sim 7 \mu\text{A}$ . The purification of the beam was obtained in two steps including laser ionization and mass-separation. Since at around  $A=80$  the only surface-ionized component of a photo-fission generated ion beam is Ga, complete isotope purity was achieved, without any contamination of  $^{80}\text{Rb}$ . This cleanness was tested by the  $\beta$ -gated  $\gamma$  spectrum. No contaminating  $\gamma$ -rays, like  $\beta^+/\epsilon$ -delayed 616.7 keV  $\gamma$ -line of  $^{80}\text{Kr}$ , were found in the spectrum other than  $\gamma$ -rays from  $^{80}\text{Ge}$  and its daughter and granddaughter nuclei. The purified  $^{80}\text{Ga}$  beam was directed and implanted on a periodically moving tape for minimizing the daughter's activity. The time settings were 0.5s for background, 5s for ion collection and 5s for decay measurement. The implantation rate was  $\sim 10^4$  pps.

The emitted radiation was detected in the BEta Decay studies at Orsay (BEDO) set-up that was mounted with one cylindrical plastic detector for  $\beta$ -tagging, surrounded by two high purity germanium detectors (HPGe) and three PARIS (Photon Array for studies with Radioactive Ion and Stable beams) clusters [20, 21]. The high energy resolution of the HPGe in the 0 - 6 MeV energy range makes very effective the  $\gamma$ - $\gamma$  coincidence technique not only to reconstruct the transition cascades but also to suppress the background drastically. PARIS has high detection efficiency in the 6 - 10 MeV. Furthermore, PARIS has capabilities of pileup rejection and vetoing of Compton-scattered escaping events, covering angles  $0^\circ$ - $56.3^\circ$  when a photon hits the center of the first crystal. Certainly, one should count the detection efficiency of the outer-layer NaI as well. Thanks to the larger volume of the outer-layer NaI crystal of  $2'' \times 2'' \times 6''$  compared to  $2'' \times 2'' \times 2''$  for the front  $\text{LaBr}_3(\text{Ce})$  crystals of a PARIS detection unit, we have higher detection efficiency in the outer-layer to perform anti-coincidence analysis. According to Klein-Nishina formula, for a  $\gamma$ -ray with energy larger than 2 MeV, the scattering cross section for an angle larger than  $56.3^\circ$  is rather small. Furthermore, the scattered photons to large angles are mainly in the 0-2 MeV energy range. Thus, the higher-energy part of the  $\gamma$  spectrum is background free. One can directly extract information avoiding the use of Monte-Carlo simulations or of any theoretical assumption for the background- $\gamma$  strength distribution. The detectors were energy calibrated up to 9 MeV using sources including  $^{152}\text{Eu}$ , AmBe and  $^{58}\text{Ni}(n_{th}, \gamma)$  with energy of 8999.267(15) keV. Eventually, the detection set-up covered the whole  $Q_\beta$  window. Therefore, a detailed spectroscopy of low- and high-energy states has been achieved.

Data were acquired in a triggerless mode. The decay level schemes were experimentally separated using the "X" method [16]. X is the fractional direct  $\beta$ -feeding from  $^{80m}\text{Ga}$ . Calculated X values of  $\beta$ -populated states could be found in Tab. 5.3 and Tab. 5.4 in Ref. [10] which were used to attribute each state to one of the two decay schemes. Levels with values  $X = 0$  are considered as candidates to the decay scheme of the longer-lived  $^{80g}\text{Ga}$  and  $X = 1$  to the decay scheme of

the shorter-lived isomer  $^{80m}\text{Ga}$ . The taken actions are: (1)  $X < 0.4$ , belong to gs decay; (2)  $X > 0.6$ , belong to isomer decay; (3)  $0.4 < X < 0.6$ , belong to both, i.e. 50% and 50%. A narrow window of cross feeding was chosen due to considering small probability of cross  $\beta$ -feeding, at least one of  $^{80g+m}\text{Ga}$  needs to take first-forbidden transition. This standard was taken for the purpose of achieving the  $\log ft$  and  $B(\text{GT})$  values with high precisions. After the analysis, only 10 states with small  $\beta$ -branching ratios were assigned to simultaneous direct  $\beta$ -feeding from both  $^{80g}\text{Ga}$  and  $^{80m}\text{Ga}$ , out of a total of 81 populated states. The second method that assists to identify the precursors is to compare the gated  $\gamma$  spectra under different conditions on  $\beta$ -activity curves. This profits from the difference in half-lives between the ground state and isomer. For example, one can put a gate on 5.5 s - 8 s (period 1), after beam collection, to obtain a gated spectrum. Next, the same operation can be taken but gated on 8 s - 10.5 s (period 2) to get another gated spectrum. Then, one can immediately observe some survived peaks in period 2 being relatively weaker than others. This demonstrates that the precursor populating these  $\beta$ -delayed  $\gamma$ -rays has a shorter half-life than the other one. This would be  $^{80m}\text{Ga}$ . The last method is to compare the relative  $\gamma$ -ray intensities in different fissioning systems as they produce different isomeric ratios. For example, through this comparison, one finds that  $^{80m}\text{Ga}$  ratio is lower in photo-fission  $^{238}\text{U}(\gamma, n_f, f)$  than in thermal neutron-induced fission  $^{235}\text{U}(n_{th}, f)$ . Therefore, if a  $\gamma$ -ray relative intensity is lower in photo-fission, one can reach the conclusion that the related state emitting this  $\gamma$ -ray was  $\beta$ -fed by  $^{80m}\text{Ga}$ .

**Results and discussion.** Formula 1 was used to extract  $B(\text{GT})$  from observed  $\log ft$  values. Note that for  $^{80}\text{Ga}$  the Fermi terms are zero as the isobaric analogue state is located above  $Q_\beta$ .

$$\begin{aligned} t_{1/2}^{-1} &= \frac{1}{K} f [g_V^2 \frac{|\langle f || \sum_{i=1}^A \tau^- || i \rangle|^2}{2J_i + 1} + g_A^2 \frac{|\langle f || \sum_{i=1}^A \sigma \tau^- || i \rangle|^2}{2J_i + 1}] \\ &= \frac{1}{K} f [g_V^2 |M_{F/GT}^{eff}|^2 + g_A^2 |M_{GT}^{eff}|^2] \\ &= \frac{1}{K} f [g_V^2 B(F) + g_A^2 B(GT)] \end{aligned} \quad (1)$$

Where  $K/(\hbar c)^6 = 2\pi^3 \hbar \ln 2 / (m_e c^2)^5 = 8120.27648(26) \times 10^{-10}$  [22],  $f$  is the Fermi integral function,  $M_{F/GT}^{eff}$  is the effective nuclear matrix element,  $g_A$  and  $g_V$  are the axial-vector and vector coupling constants in unit of Fermi constant  $G_F$ ,  $g_A/g_V = -1.2756(13)$  [23].

Fig. 1(a) and Fig. 1(b) present the cumulative  $B(\text{GT})$  up to  $S_n$  (8.08 MeV). The total  $B(\text{GT})$  within this energy window is measured to be 0.150(8) for  $^{80m}\text{Ga}$  and 0.072(3) for  $^{80g}\text{Ga}$ . The uncertainties on  $B(\text{GT})$  values originate from the uncertainties on  $Q_\beta$  value, half-lives of precursors,  $I_\beta$  and excitation energies of states. For cumulated results, the method of propagation of uncertainty was used. Our cumulative  $B(\text{GT})$  for  $^{80m}\text{Ga}$  agree with those reported in Ref. [24] up to 4.2 MeV.

For the purpose of comparison, previous results were split according to the isomer ratio in our data. Black curve should be slightly higher in Fig. 1(a) while slightly lower in Fig. 1(b) in the actual situation due to the higher isomer ratio in thermal neutron-induced fission  $^{235}\text{U}(n_{th}, f)$  than in our data. From 4.2 to 6 MeV we observe some discrepancies, while from 6.047 MeV, no GT-transitions were found in Ref. [24]. One can find that two newly measured states located just below  $S_n$  have much larger  $B(\text{GT})$  values than others although the  $I_\beta$  is not very large. It is because their Fermi integral phase spaces ( $f$ ) are smaller than for low-lying states. As a results, the  $\Sigma B(\text{GT})$  value of the present work is four times that of Hoff's. For  $^{80g}\text{Ga}$ , our result is in good agreement with the experimental data up to 5.8 MeV obtained by Hoff et al. [24]. From this energy up to 6.6 MeV, strength from our data increases up to 0.072(3); no other states with energy higher than 5.8 MeV were observed in Ref. [24]. These discrepancies are caused by lack of high-lying states and consequently overweighting  $I_\beta$  of low-lying states in Hoff's work.

Furthermore, from experimental data, one observes clear jump-structure in  $\Sigma B(\text{GT})$  functions of both precursors. These jumps can be interpreted as doorways of single-particle GT  $\beta$ -transitions, based on a single-particle picture [25], which are dominated by 1)  $\nu f_{5/2} \rightarrow \pi f_{5/2}$  (first jump); 2)  $\nu p_{3/2} \rightarrow \pi p_{3/2}$  or/and  $\nu p_{1/2} \rightarrow \pi p_{1/2}$  (second one); 3)  $\nu f_{7/2} \rightarrow \pi f_{5/2}$  or/and  $\nu g_{9/2} \rightarrow \pi g_{9/2}$  (third one), respectively.

The experimental data are compared to theoretical calculations performed within a realistic shell-model approach. In particular, we have considered a  $^{56}\text{Ni}$  core with the model space spanned by  $0f_{5/2}$ ,  $1p_{3/2}$ ,  $1p_{1/2}$  and  $0g_{9/2}$  for both protons and neutrons. The two-body matrix elements of the effective Hamiltonian have been derived, within the framework of many-body perturbation theory, starting from the CD-Bonn potential [26] renormalized by way of the  $V_{low-k}$  approach [27] with the addition of the Coulomb term for the proton-proton interaction. More precisely, the  $\hat{Q}$ -box folded-diagram approach was employed [28] including one- and two-body diagrams up to the third order in the interaction in the perturbative diagrammatic expansion of the  $\hat{Q}$  box. As regards the GT operator, it is well known that the diagonalization of the effective Hamiltonian does not produce the true nuclear wave functions, but their projections onto the selected model space. As a consequence, any bare decay operator should be renormalized by taking into account the neglected degrees of freedom. For this purpose, we use the Suzuki-Okamoto formalism [29]. This allows a derivation of the decay operator consistent with the effective Hamiltonian. Consequently, the effective charges are state dependent as can be seen from Tab. XVII of Ref. [30] where the GT matrix elements of the effective GT operator are reported together with the corresponding quenching factors. The effective Hamiltonian and GT operator so derived have already been used in Ref. [30] to study the GT and two-neutrino double- $\beta$  decay matrix element of  $^{76}\text{Ge}$  and  $^{82}\text{Se}$ . Finally, we stress that our calculation is fully microscopical. In fact, we do not resort to any empirical quenching

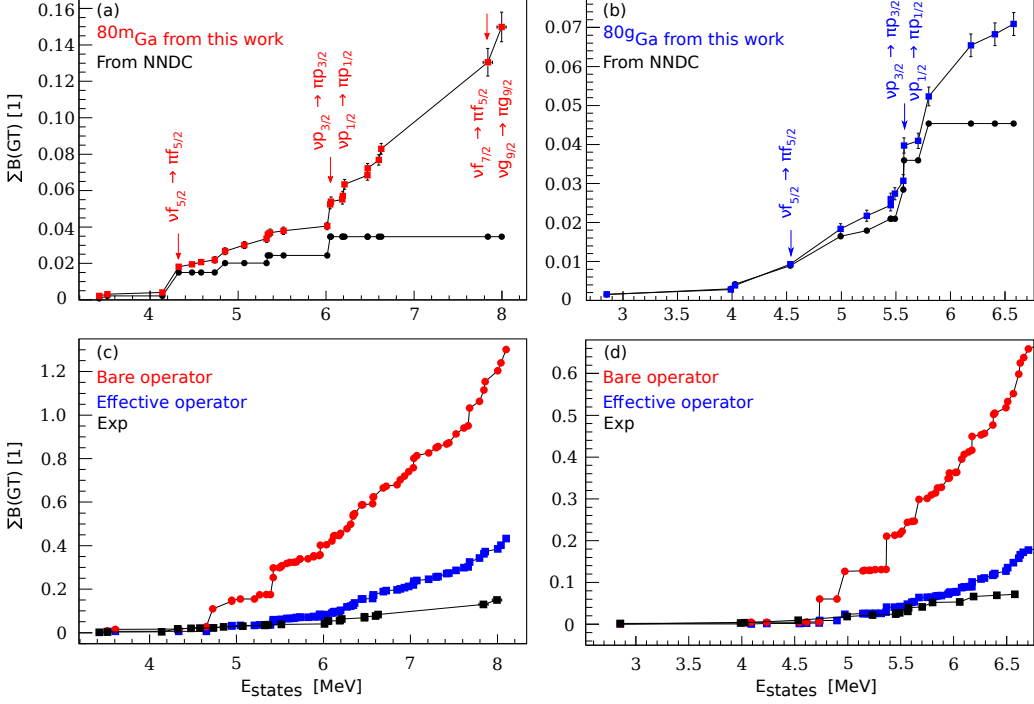


FIG. 1: (a) and (b): experimentally measured cumulative B(GT) with statistical uncertainties of  $^{80g+m}\text{Ga}$  versus excitation energy of the final states in  $^{80}\text{Ge}$ . The experimental results obtained in this work are compared to the realistic shell-model calculations performed with the bare (red dots) and with the effective GT operator (blue squares) in (c) and (d).

factor for the axial coupling constant  $g_A$ .

The microscopical nature of our calculations, and the large number of valence nucleons, may have as a consequence a not-perfect reproduction of the energy levels. Therefore, in the comparison between theoretical and experimental  $\Sigma\text{B(GT)}$  the energy of the lowest state has been shifted by 0.4899 MeV and 0.4811 MeV, respectively, for  $^{80g}\text{Ga}$  and  $^{80m}\text{Ga}$  to reproduce the energy of the corresponding experimental levels. As can be seen in Fig. 1(c) and Fig 1(d), the theoretical calculations produce similar jump structures in the running sums.

The effect of the renormalization is very evident in both cases, as it was for  $^{76}\text{Ge}$  and  $^{82}\text{Se}$  GT strength [30]. In fact, up to the region where the completeness of the experimental data is guaranteed (0-6.6 MeV), we find the theoretical strength is quenched by a factor of  $\sim 0.53$  for the isomeric state and by a factor of  $\sim 0.52$  for the ground state, respectively, under renormalization.

This strong renormalization is not surprising. In fact, while a phenomenological quenching factor of 0.744(15) for  $g_A$  is usually needed to reproduce the experimental data in the region of fp-shell nuclei [5], a higher renormalization is required in heavier-mass region nuclei as shown in a previous study [30]. This is because for the spin- and spin-isospin-dependent operators like  $\Sigma\sigma\tau^-$ , a configuration with more than one valence nucleon plays a more important role in nuclei located

in medium- and heavy-mass regions than those in light-mass region. This conclusion is consistent with observation of  $2_1^+$ -based pygmy dipole resonance that evidences collectivity in the daughter nucleus  $^{80}\text{Ge}$  [10].

However, while for  $^{76}\text{Ge}$  and  $^{82}\text{Se}$  a good agreement between theoretical and experimental data was obtained using the effective operator [30], in the present case, even in region, 0-6.6 MeV where agreement is expected, we overestimate the experimental  $\Sigma\text{B(GT)}$ . From experiment,  $\Sigma\text{B(GT)}$  are 0.083(3) and 0.072(3) for isomeric and ground states, respectively, whereas they are 0.1182 and 0.1466, respectively, from theory. This reveals the challenge in precisely reproducing the  $\beta$ -strength, especially in the low but important energy region with fine structure located within the  $Q_\beta$  window. Consequently, further renormalization of the shell-model effective GT operator is needed, probably via adding two-body [8, 9] in  $\Sigma\sigma\tau^-$  operators.

For  $\beta$  and  $\gamma$ -decay pattern analyses, due to lack of structure information of the  $4_1^+$  state and candidate  $4_2^+$  state in  $^{80}\text{Ge}$ , only decay patterns of precursor and  $\beta$ -populated states to the  $2_1^+$  and  $2_2^+$  states are analyzed. The  $2_1^+$  state has a richer multi-correlation and larger quadrupole deformation than the  $2_2^+$  state, representing higher collective excitation than the  $2_2^+$  state [15, 31]. This character was confirmed by analysis of the neutron and proton components in reproducing of the  $\text{B(E2}; 0_1^+ \rightarrow 2_1^+)$  measurement,  $A_n (<2_1^+ || \text{E2} || 0_1^+ >_n) = 13.3 \text{ e fm}^2$

and  $A_p (<2_1^+ ||E2||0_1^+ >_p) = 17.5 \text{ e fm}^2$ , respectively, while  $A_n=0 \text{ e fm}^2$  for the  $2_1^+$  state in  $^{82}\text{Ge}$  [32]. Consequently, if a precursor in  $^{80}\text{Ga}$  or a high-lying state in  $^{80}\text{Ge}$  has a large collectivity, it will have larger probability of  $\beta$ -decaying/ $\gamma$ -de-exciting to the  $2_1^+$  state than to the  $2_2^+$  state.

Figure 2 shows the  $\gamma$ - $\gamma$  matrix filled by energies of add-back-all  $\gamma$ -rays from all detectors and single  $\gamma$ -rays from HPGe detectors with coincidence time window of 50 ns. For better understanding of this, Fig. 3 presents the  $\beta$ -gated  $\gamma$  spectra measured with add-back-all mode, as shown in Fig. 2, in which energies were summed up between two HPGe detectors and twenty-seven PARIS phoswiches but on conditions of observation of 659.2 keV  $\gamma$ -ray from  $2_1^+$  state and of 915.1 keV or 1573.6 keV  $\gamma$ -ray from  $2_2^+$  state in HPGe, respectively. Therefore, these spectra present the  $\beta$ -populated excitations in  $^{80}\text{Ge}$  which de-excite to the above-mentioned two low-lying states, as illustrated by the simplified scheme in the inset of Fig. 3. Note that above 5.6 MeV only  $\beta$ -delayed  $\gamma$ -rays from  $^{80}\text{Ge}$  exist in the spectra since the  $Q_\beta$  values of the daughter nuclei of  $^{80}\text{Ga}$ ,  $^{80}\text{Ge}$  and  $^{80}\text{As}$ , are 2679(4) keV and 5545(4) keV, respectively [14]. Furthermore, since the beam was pure and anti-coincidence technique was applied via the outer-layer large NaI crystals in PARIS, the spectra are background free in the high-energy part. Random pile-up events were also removed thanks to pulse-shape discrimination function of PARIS. This is clear from the super-clean background above  $Q_\beta$  region where the statistics are constant and very low. The red curve in Fig. 3 is the statistical ratio of these two histograms where the solid line is a constant fitting between 1.8 MeV and  $S_n$ . One can observe that the ratio of these two histograms is approximately constant in a wide energy range. The value is 6.66(12). This is consistent with the parallel profiles of black and blue spectra in a global view except for some fluctuations like the peak at 4324.2 keV.

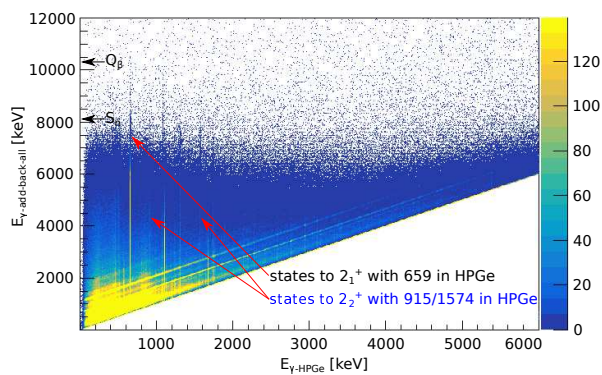


FIG. 2:  $\gamma$ - $\gamma$  matrix filled by energies of add-back-all  $\gamma$ -rays from all detectors (in PARIS, NaI crystal works as veto detector) and single  $\gamma$ -rays from HPGe detectors. X-axis values of marked lines are 659.2 keV, 915.1 keV and 1573.6 keV, respectively.

In order to obtain an accurate states-ratio between de-exciting to  $2_1^+$  and  $2_2^+$  states, populated by  $^{80m}\text{Ga}$ , cumulative  $I_\beta$  are analyzed, as shown in Fig. 4.  $\Sigma I_\beta$  of states above 2 MeV which

de-excite to  $2_1^+$  state are 22.6(10)% whereas it is 5.9(3)% for states to  $2_2^+$  state. About common states, as listed in Tab. I,  $I_\beta$ 's were separated according to  $\gamma$  branching ratio,  $R_{\gamma-(2_1^+/2_2^+)}$ . The ratio of  $\Sigma I_\beta$  is 3.83(2). Therefore, the spectrum ratio and the  $\Sigma I_\beta$  ratio both evidence that more states with  $\gamma$ -connecting to  $2_1^+$  state are populated in  $\beta$ -decay of  $^{80m}\text{Ga}$ . Simultaneously,  $\gamma$ -decay to  $2_2^+$  state results in a significant percentage/competition as well. Note that, besides influence of structure, 3.83(2) includes contribution of the factor due to the energy-gap difference between high-lying states to low-lying  $2_1^+$  and to  $2_2^+$  states [33]. For the 7 MeV state, the factor is 1.5959(4) and 2.179(1) for E1/M1 and E2/M2 transitions, respectively. The realistic shell-model calculation supports this conclusion, in which the quadrupole moments ( $Q_2^0$ ) of each state in Fig. 1(c) and Fig. 1(d) obtained with the effective operators were calculated. 52.1% of  $3^-$   $\beta$ -populated and 83.6% of  $6^-$   $\beta$ -populated states have  $Q_2^0$  values which are larger than  $10 \text{ e fm}^2$ .

TABLE I: Competitions between de-excitation to  $2_1^+$  and to  $2_2^+$  states for  $^{80m}\text{Ga}$   $3^-$   $\beta$ -populated states.

$E_{levels}$ (keV)	4324.2	5072.1	5324.5	5338.1
Br to $2_1^+$	50(1)%	76(4)%	66(7)%	51(4)%
Br to $2_2^+$	9.6(5)%	24(3)%	34(4)%	49(5)%
$R_{\gamma-(2_1^+/2_2^+)}$	5.2(3)	3.1(4)	1.9(3)	1.1(1)

For further investigating the effect of nuclear collectivity on  $\beta$ -decay property, we analyze the correlation between quadrupole deformation of precursors and relative  $\beta$ -transition strengths to highly quadrupole deformed  $2_1^+$  states in germanium isotopes. Less deformed  $2_2^+$  state was selected as a reference. In Fig. 5, the black curve presents spectroscopic quadrupole moments ( $Q_s$ ) of  $^{72g,74g,76g,78g,80m,82g}\text{Ga}$  while the red one shows the ratio of  $\log ft$  between  $2_2^+$  and  $2_1^+$  in  $^{72,74,76,78,80,82}\text{Ge}$ ,  $R_{\log ft}$ . The data point surrounded with a blue circle is from this work while others are from National Nuclear Data Center [34] and Ref. [35]. The increase of  $R_{\log ft}$  indicates that  $2_1^+$  state becomes more favored than  $2_2^+$  state, and vice versa. Therefore, if nuclear collectivity has significant impact on the  $\beta$ -decay property, the precursor with larger  $Q_s$  should have a larger  $R_{\log ft}$ . Clearly, this positive correlation has been built and is observable, as shown in Fig. 5, from  $A=74$  to  $A=82$ . However, one finds  $^{72}\text{Ga}$  is an exception that has higher  $Q_s$  but smallest  $R_{\log ft}$ . It means that it is difficult to populate states with high deformation like  $2_1^+$  state in  $^{72}\text{Ge}$  in  $\beta$ -decay due to effect of sub-shell closure at  $N=40$ . Shell structure and spherically harmonic oscillation dominate the properties of  $\beta$ -populated low-spin excitations in  $^{72}\text{Ge}$ . This evidences the significant role of nuclear shells in affecting  $\beta$ -decay property especially for stable nuclei with magic numbers in neutron or/and proton. However, the nucleus located at  $N=50$  closed shell (last data point with  $R_{\log ft}$  being larger than 1) has a different situation where nuclear collectivity has more significant impact than  $N=40$ , which could be caused by large isospin asymmetry in the neutron-rich region with

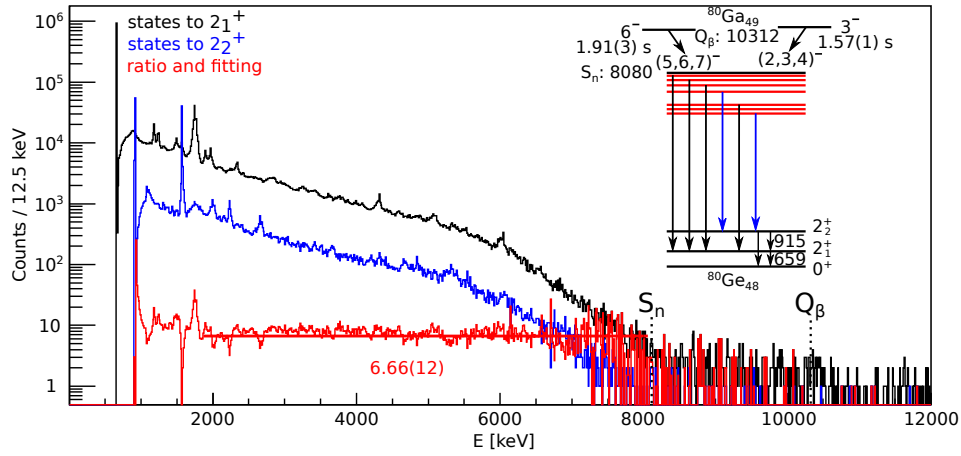


FIG. 3:  $\beta$ -gated  $\gamma$  spectra measured with add-back-all mode: black: gate on 659.2 keV  $\gamma$ -ray; blue: gate on 915.1 keV or 1573.6 keV  $\gamma$ -ray; red: ratio of black and blue histograms. Inset: simplified level scheme showing more  $\beta$ -populated states from  $^{80m}\text{Ga}$  de-exciting to  $2_1^+$  than to  $2_2^+$  in  $^{80}\text{Ge}$ .

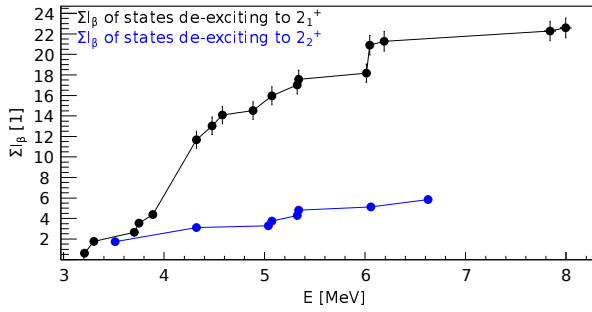


FIG. 4: Black: cumulative  $I_\beta$  of states above 2 MeV  $\beta$ -populated by  $^{80m}\text{Ga}$  which de-excite to  $2_1^+$  state; Blue: cumulative  $I_\beta$  of states,  $\beta$ -populated by  $^{80m}\text{Ga}$ , de-exciting to  $2_2^+$  state.

stronger residual interactions.

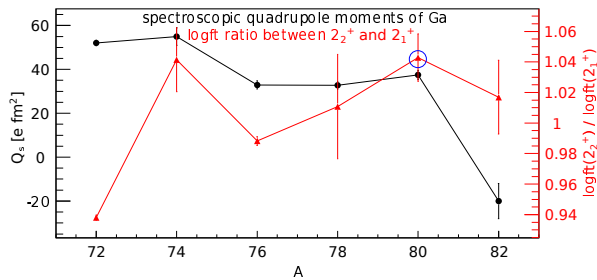


FIG. 5: Black: spectroscopic quadrupole moments of  $^{72g,74g,76g,78g,80m,82g}\text{Ga}$ ; Red:  $\log ft$  ratio of  $2_2^+$  and  $2_1^+$  states in  $^{72,74,76,78,80,82}\text{Ge}$ .

**Summary.** We have presented here experimental evidence in  $^{80}\text{Ga}$  for simultaneous impacts of nuclear shell structure, i.e. leading to jump-structure in  $\Sigma\text{B}(\text{GT})$ , and collectivity, i.e. resulting in positive correlation between deformation of precursor and selectivity to highly deformed  $2_1^+$  state, on  $\beta$ -decay property. For further justifying this conclusion, we have per-

formed a realistic shell-model calculation with the effective Hamiltonian and GT operator derived consistently within the framework of the many-body perturbation theory. Though remarkable, the renormalization is insufficient to reproduce the experimental strength, probably evidencing the need of two-body for the GT operator. Nevertheless, these results are helpful for further understanding of the quenching mechanisms of strength of the weak interaction in nuclei and, therefore, may have implications for computing the theoretical nuclear matrix elements of neutrinoless double- $\beta$  decay and for modeling r-process nucleosynthesis.

The authors thankfully acknowledge the work of the ALTO technical staff for the excellent operation of the ISOL source. R. Li acknowledges support by China Scholarship Council under Grant No.201804910509 and KU Leuven postdoctoral fellow scholarship. C. Delafosse, A. Kankainen and L. A. Ayoubi have received funding from European Union's Horizon 2020 research and innovation program under grant agreement NO. 771036 (ERC CoG MAIDEN). Use of PARIS modular array from PARIS collaboration and Ge detectors from the French-UK IN2P3-STFC Gamma Loan Pool are acknowledged.

\* Corresponding author: [liren824@gmail.com](mailto:liren824@gmail.com)

† Present address: University of Novi Sad, Faculty of Science, Novi Sad, Serbia

- [1] J. Engel and J. Menéndez, *Reports on Progress in Physics* **80**, 046301 (2017).
- [2] J. T. Suhonen, *Frontiers in Physics* **5**, 55 (2017).
- [3] J. Suhonen and O. Civitarese, *Physics Letters B* **725**, 153 (2013).
- [4] B. A. Brown and B. H. Wildenthal, *Atomic Data and Nuclear Data Tables* **33**, 347 (1985).
- [5] G. Martínez-Pinedo, A. Poves, E. Caurier, and A. P. Zuker,

- Phys. Rev. C **53**, R2602 (1996).
- [6] D. Gambacurta, M. Grasso, and J. Engel, *Physical Review Letters* **125**, 212501 (2020).
- [7] Y. F. Niu, Z. M. Niu, G. Colò, E. Vigezzi, *et al.*, *Physical Review Letters* **114**, 142501 (2015).
- [8] P. Gysbers, G. Hagen, J. D. Holt, G. R. Jansen, T. D. Morris, P. Navrátil, T. Papenbrock, S. Quaglioni, A. Schwenk, S. R. Stroberg, *et al.*, *Nature Physics* **15**, 428 (2019).
- [9] L. Coraggio, N. Itaco, G. De Gregorio, A. Gargano, Z. H. Cheng, Y. Z. Ma, F. R. Xu, and M. Viviani, *Phys. Rev. C* **109**, 014301 (2024).
- [10] R. Li, *First attempt toward a quasi-Pandemonium free  $\beta$ -delayed spectroscopy of  $^{80}\text{Ge}$  using PARIS at ALTO*, Thesis, Université Paris-Saclay (2022).
- [11] A. Algora, E. Ganioglu, P. Sarriguren, V. Guadilla, L. Fraile, E. Nacher, B. Rubio, J. L. Tain, J. Agramunt, W. Gelletly, *et al.*, *Physics Letters B* **819**, 136438 (2021).
- [12] J. A. Briz, E. Nacher, M. J. G. Borge, A. Algora, B. Rubio, P. Dessagne, A. Maira, D. Cano-Ott, S. Courtin, D. Escrig, *et al.*, *Physical Review C* **92**, 054326 (2015).
- [13] E. Nacher, A. Algora, B. Rubio, J. L. Tain, D. Cano-Ott, S. Courtin, P. Dessagne, F. Maréchal, C. Miehé, E. Poirier, *et al.*, *Physical Review Letters* **92**, 232501 (2004).
- [14] M. Wang, W. J. Huang, F. G. Kondev, G. Audi, and S. Naimi, *Chinese Physics C* **45**, 030003 (2021).
- [15] H. Iwasaki, S. Michimasa, M. Niikura, M. Tamaki, N. Aoi, H. Sakurai, S. Shimoura, S. Takeuchi, S. Ota, M. Honma, *et al.*, *Physical Review C* **78**, 021304 (2008).
- [16] D. Verney, B. Tastet, K. Kolos, F. Le Blanc, F. Ibrahim, M. C. Mhamed, E. Cottreau, P. V. Cuong, F. Didierjean, G. Duchêne, *et al.*, *Physical Review C* **87**, 054307 (2013).
- [17] B. Cheal, J. Billowes, M. L. Bissell, K. Blaum, F. C. Charlwood, K. T. Flanagan, D. H. Forest, S. Fritzsche, C. Geppert, A. Jokinen, *et al.*, *Physical Review C* **82**, 051302 (2010).
- [18] R. Lica, N. Marginean, D. G. Ghita, H. Mach, L. M. Fraile, G. S. Simpson, A. Aprahamian, C. Bernards, J. A. Briz, B. Bucher, *et al.*, *Physical Review C* **90**, 014320 (2014).
- [19] F. Ibrahim, D. Verney, M. Lebois, B. Roussière, S. Essabaa, S. Franchoo, S. Gales, D. G. Mueller, C. Lau, F. L. Blanc, *et al.*, *Nuclear Physics A* **787**, 110 (2007), proceedings of the Ninth International Conference on Nucleus-Nucleus Collisions.
- [20] M. Ciemała, D. Balabanski, M. Csatlós, J. M. Daugas, G. Georgiev, J. Gulyàs, M. Kmiecik, A. Krasznahorkay, S. Lalkovski, A. Lefebvre-Schuhl, *et al.*, *Nuclear Instruments and Methods in Physics Research Section A: Accelerators, Spectrometers, Detectors and Associated Equipment* **608**, 76 (2009).
- [21] C. Ghosh, V. Nanal, R. G. Pillay, K. V. Anoop, N. Dokania, S. Pal, M. S. Pose, G. Mishra, P. C. Rout, S. Kumar, *et al.*, *Journal of Instrumentation* **11**, P05023 (2016).
- [22] J. C. Hardy and I. S. Towner, *Physical Review C* **102**, 045501 (2020).
- [23] R. L. Workman and Others (Particle Data Group), *PTEP* **2022**, 083C01 (2022).
- [24] P. Hoff and B. Fogelberg, *Nuclear Physics A* **368**, 210 (1981).
- [25] H. Grawe, *Lect. Notes Phys.* **651**, 33 (2004).
- [26] R. Machleidt, *Physical Review C* **63**, 024001 (2001).
- [27] S. Bonger, T. T. S. Kuo, and L. Coraggio, *Nuclear Physics A* **684**, 432 (2001).
- [28] L. Coraggio, A. Covello, A. Gargano, N. Itaco, and T. T. S. Kuo, *Annals of Physics* **327**, 2125 (2012).
- [29] K. Suzuki and R. Okamoto, *Progress of Theoretical Physics* **93**, 905 (1995).
- [30] L. Coraggio, L. De Angelis, T. Fukui, A. Gargano, N. Itaco, and F. Nowacki, *Physical Review C* **100**, 014316 (2019).
- [31] D. Rhodes, B. A. Brown, A. Gade, S. Biswas, A. Chester, P. Farris, J. Henderson, A. Hill, J. Li, F. Nowacki, *et al.*, *Physical Review C* **105**, 024325 (2022).
- [32] E. Padilla-Rodal, A. Galindo-Uribarri, C. Baktash, J. C. Batchelder, J. R. Beene, R. Bijker, B. A. Brown, O. Castaños, B. Fuentes, J. G. del Campo, *et al.*, *Phys. Rev. Lett.* **94**, 122501 (2005).
- [33] W. D. Hamilton, ed., *The Electromagnetic Interaction in Nuclear Spectroscopy* (North-Holland, Amsterdam-Oxford, 1975).
- [34] Brookhaven National Laboratory, “Ensd, national nuclear data center,” <https://www.nndc.bnl.gov/ensdf/> (2024).
- [35] U. Silwal, *Detailed  $\beta$ -Decay Studies of Neutron-Rich 74-77Ga Isotopes* (Mississippi State University, 2018).